

## Article

# Numerical Study on the Impact of Gap between Sheets on the Quality of Riveted Single-Strap Butt Joints

Zhenzheng Ke<sup>1,2</sup>, Yongliang Zhang<sup>2,3</sup>, Yuchi Liu<sup>2</sup>, Zhengwei Zhong<sup>2</sup>, Chunrun Zhu<sup>2</sup> and Yunbo Bi<sup>1,2,\*</sup> 

<sup>1</sup> State Key Laboratory of Fluid Power and Mechatronic System, College of Mechanical Engineering, Zhejiang University, Hangzhou 310027, China; kzzcaen@zju.edu.cn

<sup>2</sup> Key Laboratory of Advanced Manufacturing Technology of Zhejiang Province, College of Mechanical Engineering, Zhejiang University, Hangzhou 310027, China; zhangyl009@avic.com (Y.Z.); liuyuchi@zju.edu.cn (Y.L.); 21825217@zju.edu.cn (Z.Z.); zjuzcr@zju.edu.cn (C.Z.)

<sup>3</sup> Aviation Industry Corporation of China Shenyang Aircraft Corporation, Shenyang 110850, China

\* Correspondence: zjubyb@zju.edu.cn

**Abstract:** Some controllable process parameters in the riveting process such as the gap between sheets, have an important impact on the quality of a riveted butt joint. In this paper, the finite element model of a riveted single-strap butt joint is established with the help of ABAQUS analysis software, and the riveting process is simulated under five kinds of gaps between sheets. From the perspectives of rivet upsetting size, rivet interference, radial deformation of sheet, and analysis of residual stress around the hole of sheet, the influence of the gap between sheets on the connection quality of the riveted butt joint is summarized. The results show that the left and right sheets will contact each other and there is extrusion stress between the sheets when the gap is zero. When the applied tensile load continues to increase, due to the influence of the secondary bending, the strap sheet responsible for the connection produces warping deformation, and there will be no further contact between the sheets. When the gap between sheets increases from 0 to 2 mm, the maximum deformation of strap sheets increases from 0.876 to 0.927 mm, which proves that the gap between sheets have no significant effect on the deformation of the strap sheet.

**Keywords:** single-strap butt joints; gap between sheets; riveting quality; finite element model



**Citation:** Ke, Z.; Zhang, Y.; Liu, Y.; Zhong, Z.; Zhu, C.; Bi, Y. Numerical Study on the Impact of Gap between Sheets on the Quality of Riveted Single-Strap Butt Joints. *Coatings* **2021**, *11*, 1375. <https://doi.org/10.3390/coatings11111375>

Academic Editor: Grzegorz Dercz

Received: 29 September 2021

Accepted: 7 November 2021

Published: 10 November 2021

**Publisher's Note:** MDPI stays neutral with regard to jurisdictional claims in published maps and institutional affiliations.



**Copyright:** © 2021 by the authors. Licensee MDPI, Basel, Switzerland. This article is an open access article distributed under the terms and conditions of the Creative Commons Attribution (CC BY) license (<https://creativecommons.org/licenses/by/4.0/>).

## 1. Introduction

The mechanical connections used in aircraft assembly are riveted, welded, glued, or mixed connections. According to relevant data, riveting and bolting methods account for more than 70% of aircraft structural connection methods, and the workload of riveting accounts for about 20%–30% of the total aircraft work [1,2]. The riveting process has the characteristics of reliable connection, low cost, easy troubleshooting, and is suitable for connection between metal and non-metal materials. With the development and popularity of automatic drilling and riveting technology, the efficiency and quality of riveting processing have improved significantly, which has promoted the development and application of riveting technology.

The connection quality of riveted parts has an important impact on the development of the aviation industry, failure of riveted structures is one of the most common causes of failure in aircraft [3–5]. A total of 70% of aircraft fuselage fatigue failures occur in the structural connection area, with 80% of the cracks occurring at the connection holes [6]. For example, a Boeing 737 of Aloha Airlines had an airborne disintegration accident during a flight due to rivet fatigue failure [1], and a F-111 fighter jet of the U.S. Army crashed during a flight due to fatigue failure at the rivets that caused the wing to fall off [7]. Therefore, it is crucial to improve the quality of riveting during aircraft assembly.

As a docking connection method, butt connection is widely used in the assembly connection of fuselage and wing of aircraft. Figure 1 shows the schematic diagram of

the docking structure section of the tail section and the rear section of a transporter. The conveyor adopts the butt connection, and the strap sheet is used to connect the backbox and the tail section [8]. The gap between sheets is a potential influencing factor that needs to be considered. In the riveting process, due to the existence of residual stress, the strap sheet will have a certain degree of deformation in the axial and radial directions after the riveting is completed. When the gap between sheets is too small, there may be collision extrusion between the panels under the action of tensile load, thus affecting the connection quality of the panel connector. Therefore, it is necessary to do further research on such issues.

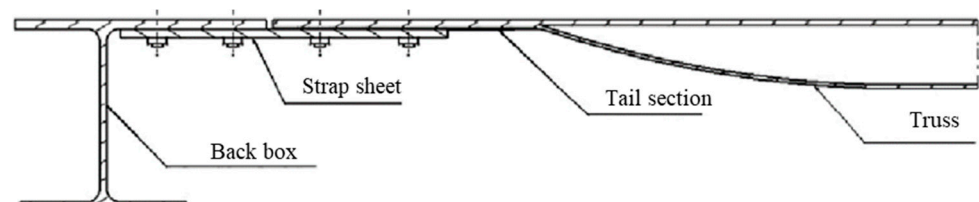


**Figure 1.** The tail end of the fuselage and the rear section of the strap sheet connection schematic.

The study of the strength and fatigue life of riveted single-strap butt joints has been the focus of scholarly research. Szolwinski et al. [9] found that the compression riveting force affected the stress distribution around the rivet hole, and that the expansion of fatigue cracks at and around the nail/hole interface was related to the residual stress field generated during the riveting process. The occurrence of fatigue damage in riveted structures was related to the stress gradient generated by the contact between the rivet and the rivet hole. Atre et al. [10] investigated the distribution of stresses and strains around the rivet hole by means of finite element simulation. Aman et al. [11] investigated the optimal riveting sequence to reduce residual stresses and improve the quality of riveted joints utilizing finite element simulation. Manes et al. [12] investigated the riveting process in terms of the compression rivet force, the rivet length, and rivet and sheet hole diameter tolerances on the riveted joint quality, and the results showed that the compression force had the greatest effect on the riveted fatigue. Yu et al. [5] used the numerical method to study the comprehensive effect of residual stresses caused by rivet patterns and pitches on the local stress of riveted lap joints. The smaller rivet pitch produces higher compressive residual stresses at the edge of rivet holes, which is conducive to the fatigue performance of riveted joints. Kumar et al. [13] conducted nonlinear finite element analysis on riveted lap joints and found that as long as the rivet did not yield, the load distribution between rivets was not uniform, which may lead to local high stress and cracking. Liu et al. [14] numerically studied the residual stresses distribution of single-band butt joints with different rivet sizes and thicknesses. There is little research on the influence of gap between sheets on riveting quality.

The use of multiple rows of rivets in a strap sheet connection generally results in uneven loading of the rivets, resulting in large rivet loads at both ends, which becomes a weak link in the performance of the joint [15]. For the strap sheet connection, when the gap between the sheets is set too small, the sheets will be in contact with each other after the riveting is completed, thus affecting the stress distribution between the sheets.

In this paper, the influence of the gap between sheets on the connection quality of single-strap butt joint is studied by numerical simulation. The finite element model of strap joint is established by using ABAQUS finite element analysis software. Referring to the published literature, reasonable boundary conditions, contact, and analysis steps are set according to the riveting process, and the finite element numerical simulation of riveting and loading process is carried out. The simulation results are analyzed to summarize the influence of the gap between strap sheets on the connection quality and mechanical properties of butt connectors.

## 2. Finite Element Model of Single-Strap Butt Joint

Since riveting is a highly nonlinear problem among multiple objects with complex contact, the ABAQUS/Explicit algorithm is used to simulate the influence of the gap between riveted strap sheets on the quality of joint [16]. Considering factors such as computational accuracy and computational time of finite element simulation, it is necessary to make appropriate simplifications in the establishment of the simulation model as well as the calculation under the premise of meeting the requirements [17]. The local simplification of the annular joint with strap sheet connection structure is shown in Figure 2. The inner and outer parts of the sheet connection part are two curved surfaces, and the studied area is a part of the strap sheet connection structure due to the large radius of curvature of the surface, so the object of study is simplified to the connection of two flat sheets.

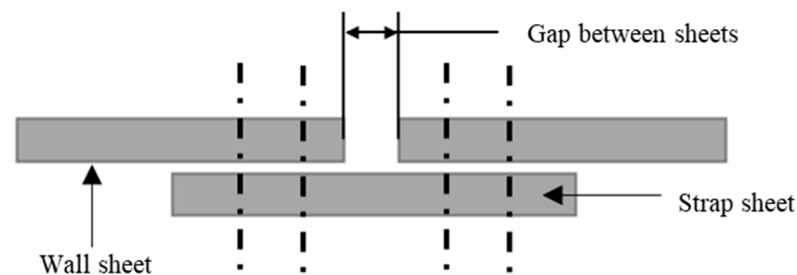


Figure 2. Schematic diagram of single-strap butt joint.

Considering the symmetry of the structure, both wall sheets will be deformed after the riveting is completed. The seam gap scheme is designed as shown in Table 1, and the finite element simulation of compression riveting and tension is done for the five groups of riveted joints [18].

Table 1. Groups of the gap between sheets.

Group	1	2	3	4	5
Gap between sheets/mm	0	0.1	0.2	1	2

The diameter of the rivet can be calculated from Equation (1) [19]:

$$d \geq 2\sqrt{\sum \delta} \quad (1)$$

where  $\sum \delta$  is the total thickness of the strap sheets.

In this paper, using the 4 mm diameter rivet, the length of the rivet can be calculated using Equation (2) [19]:

$$l = d + 1.2\sum \delta \quad (2)$$

where  $d$  is the diameter of the rivet,  $l$  is the length of the rivet.

The finite element simulation model of the strap sheet joint consists of the left wall sheet, right wall sheet, strap sheet, rivet, rivet die, and other parts, and the specific parameters and model of the joint are shown in Figure 3. In the process of finite element analysis, the material properties will affect the accuracy of the calculation results. The material of the strap joint is aluminum alloy, the material of the left and right wall sheets and strap sheets is AL2024-T3, and the rivet is a countersunk head rivet of standard grade YSA622-100°, the material of which is 2117-T4 aluminum alloy, and the chain riveting is used, and the rivets of adjacent rows are located in the same transverse line. The rivet die is set as a rigid body due to its small deformation relative to the other parts. The material property parameters mainly include density, modulus of elasticity, Poisson's ratio, yield strength and intrinsic structure relationship model, etc. The specific parameters are shown in Table 2 [20] and the

stress–strain relationship is shown in Figure 4. The constitutive relationship model can be described by the power exponent hardening model  $\sigma_{true} = C \cdot \epsilon_{true}^r$ .

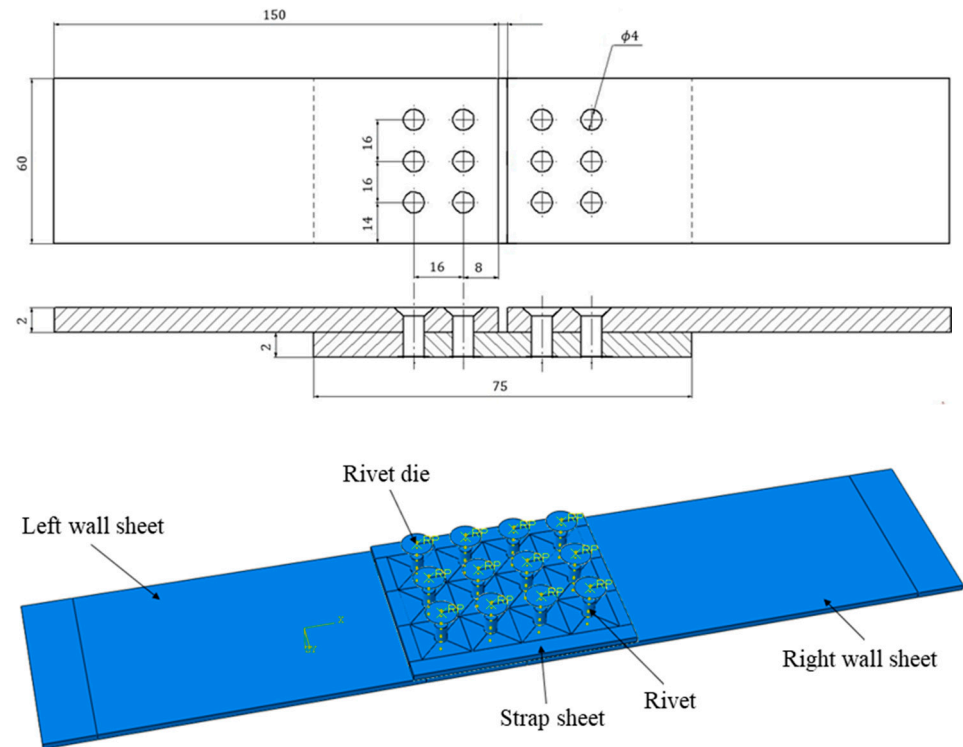


Figure 3. Schematic diagram of the dimensions and finite element models of the single-strap sheet connection joint.

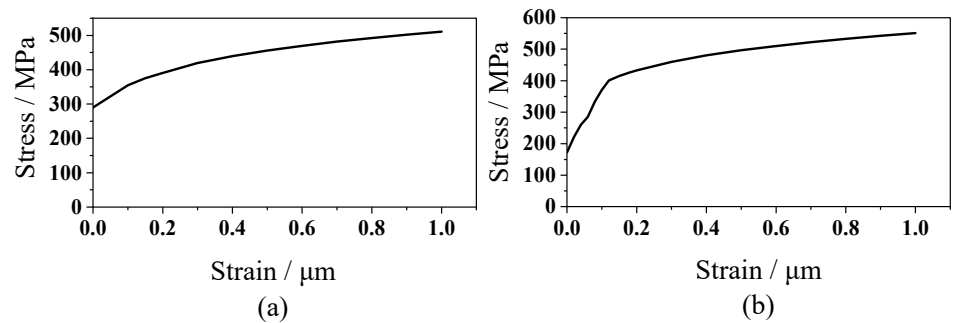


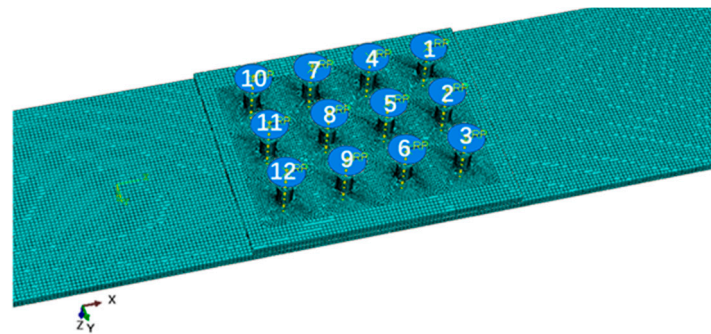
Figure 4. The stress–strain relationship of materials used in modeling. (a) AL2117-T4; (b) AL2024-T3.

Table 2. Material properties for rivet and sheets used in modeling.

Material	Elastic Modules/MPa	Poisson Ratio	Yield Strength/MPa	Density/(kg/cm <sup>3</sup> )
AL2117-T4	71,700	0.33	480	2690
AL2024-T3	72,400	0.33	310	2730

In this paper, C3D8R cells are used for the rivet, wall sheet, and strap sheet meshes, and since the main focus is on the stress distribution around the rivet, the mesh sparse division technique is used in the finite element simulation to divide the mesh with different densities for different regions, which can reduce the scale of the analysis while ensuring the computational accuracy. The riveting analysis is a complex nonlinear contact problem with high computational cost, and the plastic deformation during riveting is mainly concentrated at the rivet and 2.5 times the radius of the rivet around the hole of the connected part [21].

In order to improve the simulation accuracy and computational efficiency, the mesh around the rivet hole is refined, we subdivide the square area grid with the center of the rivet as the center and the edge length of four times the diameter of the rivet. There are 3600 mesh elements in each square area, and 43,200 mesh elements in the unilateral experimental sheet. The mesh in other parts can be appropriately sparse, and the simulation model after meshing is shown in Figure 5.



**Figure 5.** Schematic diagram for Meshing Model of riveted single-strap butt joints.

Finite element simulation analysis steps include riveting steps and tensile steps. For the joint shown in Figure 5, rivets No. 1 to No. 12 in sequence are riveted to obtain riveted parts. According to the motion law of riveting process [21], the process of single rivet riveting is divided into the loading process and the unloading process. The riveting process is a process of forming high-speed and high-strain impact load, and the Explicit analysis module in ABAQUS 6.14 is used for simulation.

**Stage 1: Loading process.** Start with the riveting die at the initial position until the riveting die moves to the maximum riveting distance. This stage is the main stage of the riveting process. During the loading process, the rivet is compressed and deformed to form the upset head. Single rivet loading process analysis step time is 1 ms [19].

**Stage 2: Unloading process.** Starting from the rivet die movement to the maximum riveting distance, the die retraction motion is set. The die is separated from the header and continues to retreat to a certain distance. The analysis step time of the unloading process for a single rivet is 1 ms [19]. The stretching simulation step is performed on the basis of the riveting completion.

**Stage 3: Tensile process.** Remove the constraint of the rivet head and the clamping constraint of one end, apply the X-direction tensile load to the original wall clamping part. The tensile analysis step uses the prevention method of force load control, and the maximum tensile load is set at 25 KN. At the beginning of the tensile analysis step, a large value will be set. After many simulations, it can be found that the rivets have all broken around 4 ms, and the wall sheet on one side is separated from the strip sheet. Therefore, the time of the tensile analysis step is set to 5 ms. The tensile load is set to linear growth, the initial value is 0, and reaches the maximum at 5 ms.

Appropriate simplifications were made in setting the boundary conditions. Limiting the degrees of freedom of the rivet head simulates the clamping of the presser foot during the riveting process. Restrict the freedom of the two ends of the sheet to simulate the clamping of the workpiece during riveting. The model boundary conditions and degrees of freedom settings are shown in Figure 6. In riveting operation, fix both ends clamping area and pressing foot area. In the tensile simulation step, the clamping constraint at one end and the constraint at the rivet are canceled, and the X-direction stretching force is applied instead.

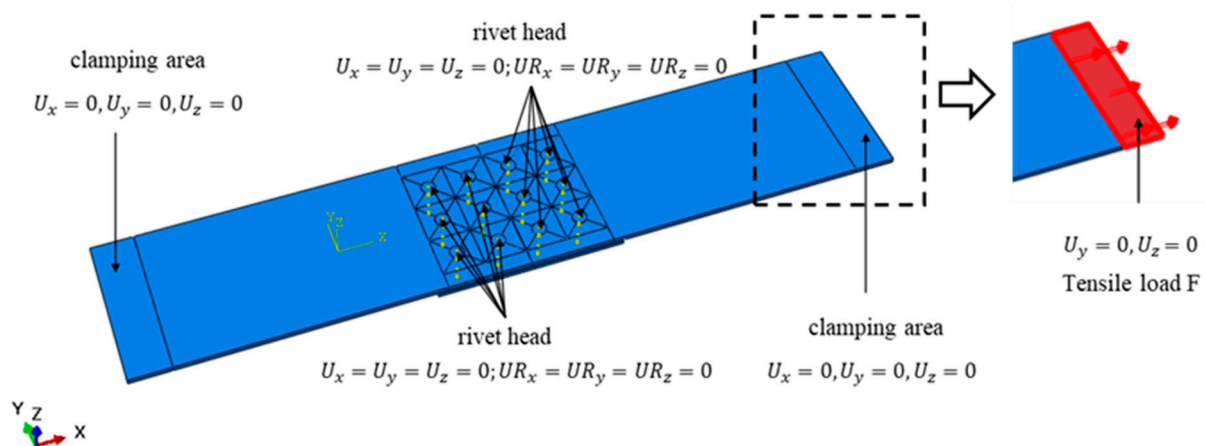


**Figure 6.** Boundary condition setting for riveting with sheet metal.

ABAQUS can be used for motion control by force and displacement loads. In this paper, the rivet riveting is controlled by displacement, and the motion displacement of the riveting die in the Z direction is set in the load module. According to the principle of volume conservation of rivets, the riveting pressure can be calculated by Equation (3) [11]:

$$S \approx L_2 - (t_1 + t_2 - t_3) - \frac{d^2 L_2 - d_3^2 (t_1 + t_2 - t_3)}{D_p^2} \quad (3)$$

where  $L_2$  is the length of the nail bar,  $t_1$  is the thickness of the wall sheet,  $t_2$  is the thickness of the strap sheet,  $t_3$  is the height of the nail head,  $d$  is the diameter of the rivet,  $d_3$  is the diameter of the wall sheet hole,  $D_p$  is the diameter of the header after riveting. Substituting the corresponding parameters into the calculation, the lower pressure of the rivet die can be obtained as 3.71 mm.

According to the analysis of riveting process [21], the contact pairs in the model can be summarized as follows:

- (1) Contact between the lower surface of the riveting die and the side face of the rivet rod.
- (2) Contact between rivet cylindrical surface and sheet hole.
- (3) Contact of rivet cylinder and sinker cone with panel hole wall and sinker hole.
- (4) Contact between wall sheet and strap sheet.
- (5) Contact between upsetting head surface and wall sheet surface after rivet deformation.
- (6) Contact between left and right wall sheet.

The above contact pairs are set to General contact in ABAQUS, and there is friction between the contact surfaces. Because the friction has little effect on the calculation results, the friction coefficient is set to 0.2 [22]. The whole finite element simulation process takes 2 h and 40 min finally.

### 3. Results and Discussion

#### 3.1. Analysis of the Effect of Butt Gap on Riveting Performance

##### 3.1.1. Analysis of Rivet Interference

Interference is an important indicator to evaluate the riveting quality [23]. If there is a certain amount of interference in the connection hole, a large residual compressive stress will be generated on the wall of the hole. When loading the connection, due to a radial compressive stress and tangential tensile stress around the hole at the same time, the stress direction at the connection joint is opposite, so that the stress level on the connector is greatly reduced, thereby improving the fatigue strength of the connection. The path function in ABAQUS finite element software was used to observe the distribution of interference along the thickness direction of the rivet. The path was set at the edge of the rivet hole, as shown in Figure 7.

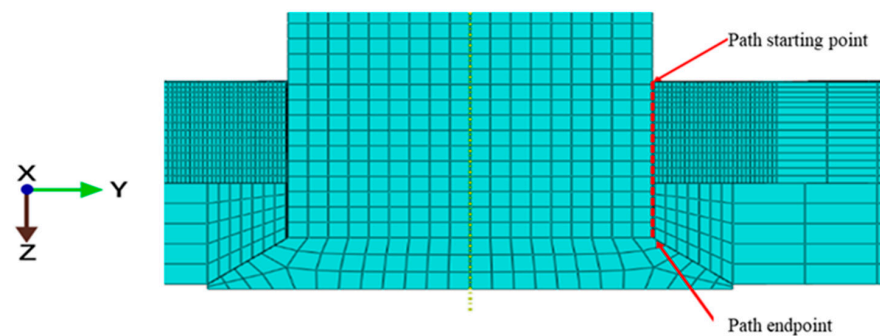


Figure 7. Rivet interference path position.

The interference distribution along the rivet thickness direction of connectors with different clearances is shown in the Figure 8. The interference amount is unevenly distributed along the rivet thickness direction, and increases nonlinearly with the increase of the gap between the joints. The interference of the rivet head side is greater than that of the sink head side. The interference of rivets on the upsetting head side is large, which is due to the upsetting head formed by the deformation of the nail rod side during the riveting process, which has a large extrusion effect on the rivet hole.

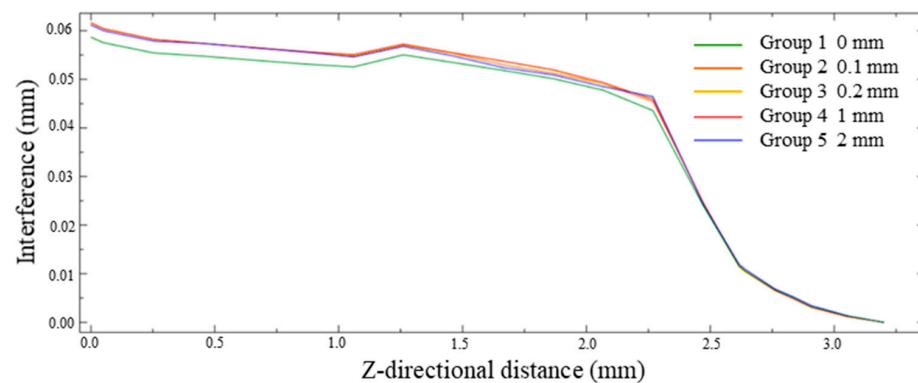


Figure 8. Distribution of rivet interference in joints with different gaps.

With the increase of Z-direction distance, the interference decreases, and the change of interference is relatively stable in the range of 0 to 2.25 mm. However, it decreases rapidly in the range of 2.25 to 2.6 mm, and finally the interference at the countersink is very small, not exceeding 0.01 mm. Compared with the interference distribution of the plate connector with different gaps, the interference of the connector is the smallest when the gap is 0, the maximum is 0.058 mm, and the interferences of the rivet of the butt joints with the gap of 0.1 to 2 mm are almost the same.

### 3.1.2. Analysis of Sheet Boundary Deformation

The deformation of riveted sheet is related to the diameter and number of rivets and the diameter of hole. According to the position shown in Figure 9, path 1, path 2, path 3 are set to observe the strain distribution of the sheet boundary after riveting. The path view is along the Y direction. Path 1 run along the top sheet, and path 3 run along the bottom sheet. The rivet interference of the Y-direction path is shown in Figure 10. The interference of rivet is 0.01 mm in the range of 0 to 2.25 mm, and the interference of rivet in path 1 on the upper surface of the sheet is 0.005 mm less than in path 3 on the lower surface of the sheet. There are two rows of rivets on each sheet. The uneven deformation of the sheet section is the superposition of the interference between the rivet and the sheet.

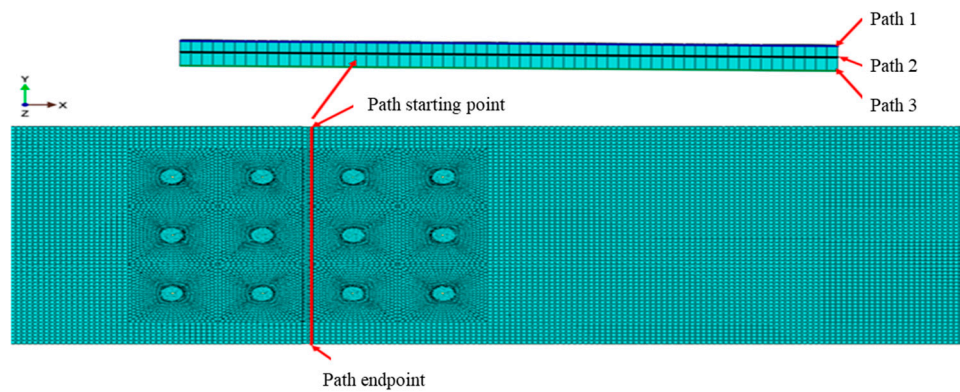


Figure 9. Path location of sheet boundary.

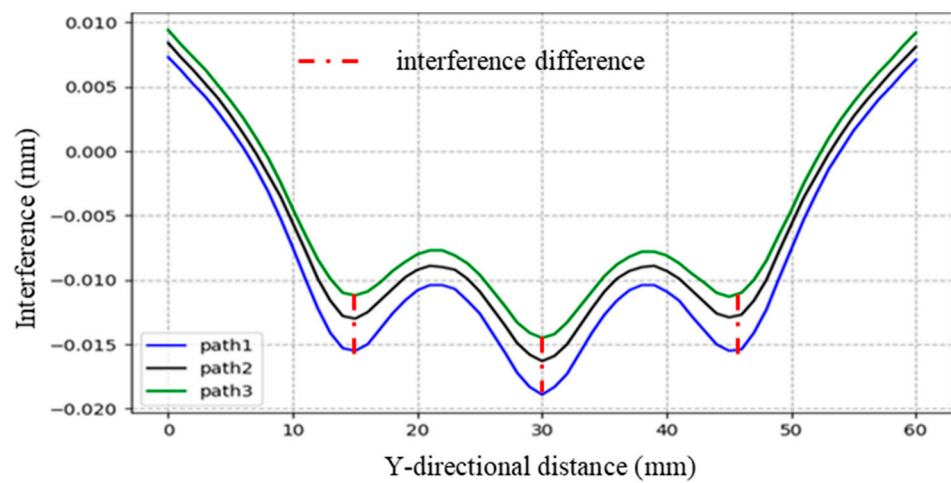


Figure 10. The rivet interference of the Y-direction path.

The X-direction deformation of the sheet after riveting is shown in Figure 11. For the three-row rivet connector, the radial deformation of the wall sheet around the hole of the middle rivet is slightly larger than that of the two sides. For the same side of the panel, the radial deformation of the panel from top to bottom decreases in turn. The radial deformation of the middle rivet is larger, and the radial deformation value is about 0.02 mm. The radial deformation of the wall sheet may be affected by the rivet interference, and the middle rivet is superimposed by the deformation of the rivet on both sides except itself. The deformation of rivets on both sides only includes the influence of their own deformation and the deformation of intermediate rivets, so the deformation of rivets on both sides is smaller than that of intermediate rivets.

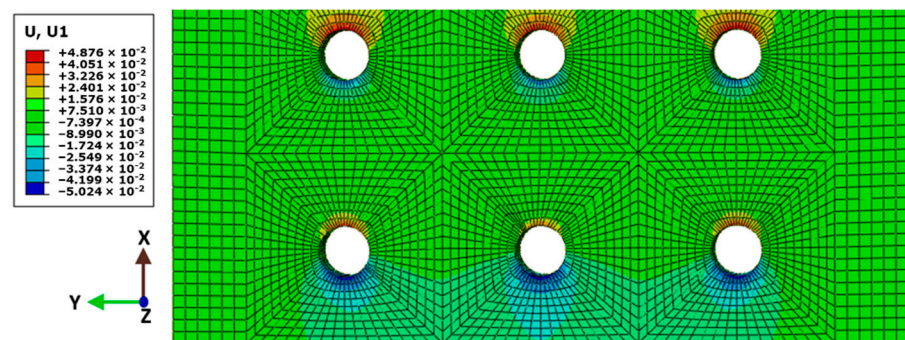


Figure 11. Deformation of X-direction riveted sheet.

The boundary deformation of the wall sheet after riveting is completed for different butt gaps is shown in Figures 12 and 13. When the butt gap between the wall sheets is 0, the displacement at the end of the wall sheets is 0 for the 10 to 50 mm section, while the trend at the boundary of the wall sheets is approximately the same when the butt gap between the wall sheets is 0.1 to 2 mm. The maximum deformation after riveting is approximately 0.018 mm for one side of the wall sheet and 0.036 mm for both sides of the wall sheet. A joint with a 0 seam gap has the wall sheets touching each other after riveting and the wall sheets are limited to displacement in the x-direction. Whereas when the gap between the wall sheets is between 0.1 and 2 mm, no contact occurs between the wall sheets after riveting.

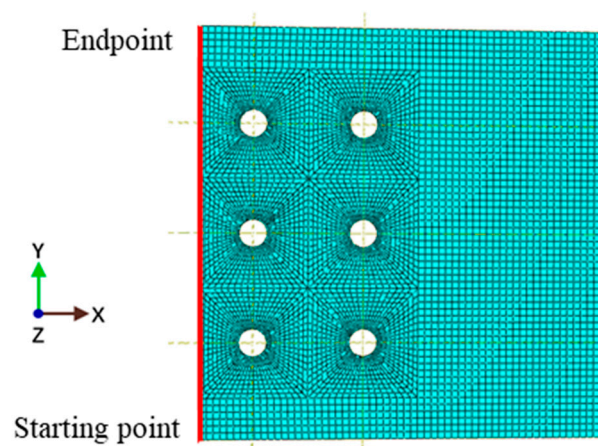


Figure 12. Observation path of the wall sheet.

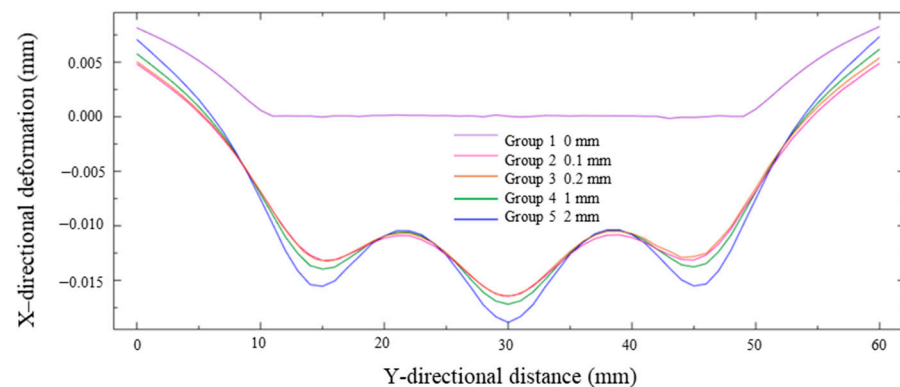
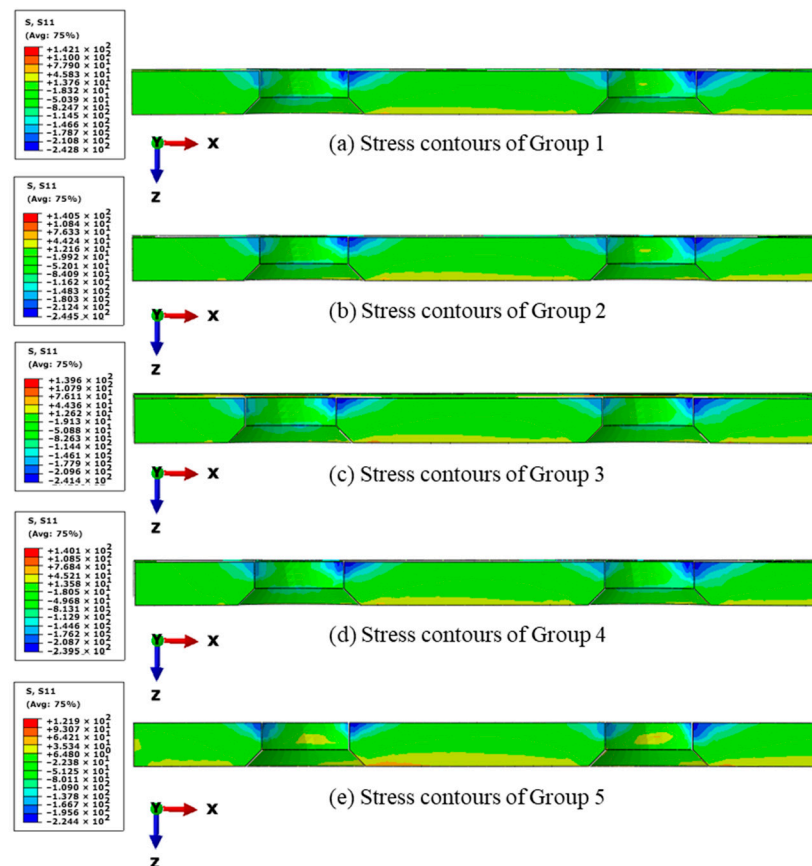


Figure 13. Boundary deformation of the wall sheet after riveting.

### 3.2. Analysis of the Influence of the Butt Gap on the Tensile Properties of Strap Sheet Joints

#### 3.2.1. Analysis of Sheet Stress

When the X-direction tensile load is applied after the riveting is completed, there may be contact between the joint sheets, resulting in extrusion, which affects the deformation and stress distribution of the sheets, with the area where the extrusion occurs being mainly at the adjacent boundary of the wall sheet. The stress distribution in the middle section of the plate along the X-direction after riveting is completed with different butt gaps is shown in Figure 14, and the group can be seen in Table 1. There is little difference in the stress distribution in the cross-section of the plate with different butt gaps. After riveting the joint with a 0 gap, there is an extrusion stress between the wall sheets due to the small gap value. With a gap of 0.1, 0.2, 1, and 2 mm, the sheets are not subjected to tensile loading and therefore do not affect the stress distribution in the joint.



**Figure 14.** Stress contours of the wall sheet (Unit: MPa). (a) Stress contours of Group 1. (b) Stress contours of Group 2. (c) Stress contours of Group 3. (d) Stress contours of Group 4. (e) Stress contours of Group 5.

In order to more intuitively observe the stress distribution and deformation of rivet and panel during the tensile process, the model is sliced along the centerline of the intermediate rivet. Figure 15 shows the stress contours of riveted lap joints under different gap clearances after riveting and tensile processes. The maximum stress mainly occurs at the contact corner between the driven head and the strap sheet, and there is no relationship between the stress and the gap between the joints. However, with the increase of the tensile load, the secondary bending effect can be observed [24]. At this time, the strap sheet and the wall sheet warping deformation, the wall sheet is no longer maintained in the same plane, so there is no extrusion deformation between the wall sheet.

When tension is carried out under a low strength load, the left and right wall sheets will contact each other when the gap between the sheets is 0, and there is extrusion stress between the wall sheets. When the applied tensile load continues to increase, due to the influence of the secondary bending, the strap sheet responsible for connecting produces warping deformation, and the wall sheet will not contact again. When the gap between the sheets is 0.1 to 2 mm, there is no contact between the left and right wall panels in the whole riveting and stretching simulation process.

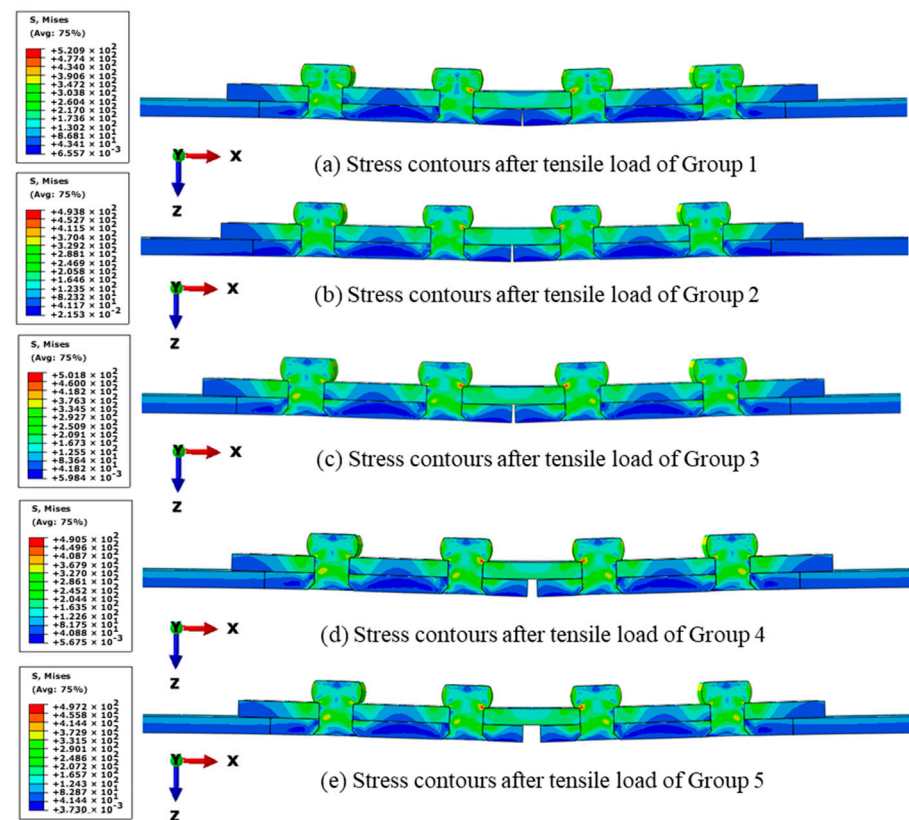


**Figure 15.** Stress contours of the riveted single-strap butt joints after tensile load (Unit: MPa). (a) Stress contours of Group 1. (b) Stress contours of Group 2. (c) Stress contours of Group 3. (d) Stress contours of Group 4. (e) Stress contours of Group 5.

### 3.2.2. Analysis of Strap Sheet Deformation

The deformation of a strap sheet under tensile load (which can be seen in Figure 6) will bend in the Z direction, which may adversely affect the quality of the riveted joint. The deformation of the strap with 0 gap under tensile load is shown in Figure 16. The deformation of the strap sheet is similar to the shape of a “U”, with a large deformation in the middle and a small deformation at the ends. The maximum deformations of strap sheets under different clearances are shown in Table 3. The larger the gap, the greater the deformation of the strap during stretching. The maximum deformation in the Z-direction of the strap is 0.876 mm for a 0 gap and 0.927 mm for a 2 mm gap.

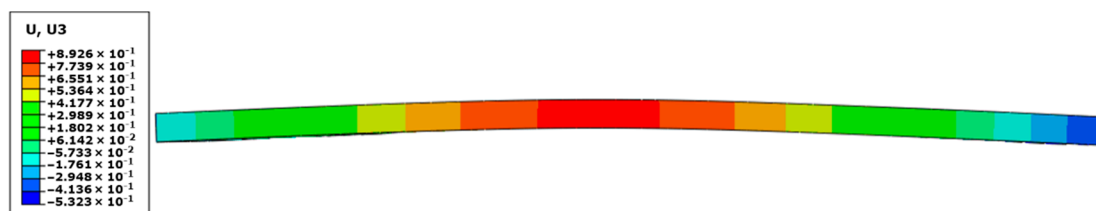


**Figure 16.** The deformation diagram of strap sheet with 0 gap. (Unit: mm).

**Table 3.** Maximum deformation of strap sheets under different gaps.

Gap between Sheets/mm	0	0.1	0.2	1	2
Max deformation/mm	0.876	0.881	0.889	0.912	0.927

During the tensile of the joint, the same fixed restraint and tensile load are applied to the joint with different butt gaps. With the same dimensional parameters of the wall

sheet and the strap sheet, the overall length of the joint grows as the gap between the joints increases and the overall bending deformation of the joint increases. Therefore, in the case of strap sheet connectors, the degree of bending deformation of the strap sheet and the degree of warpage of the wall sheet increases as the gap between the wall sheets increases.

### 3.2.3. Load Transfer Ratio Analysis of Rivet

As the contact surface between the rivet and the wall plate was previously defined, the rivet contact force CFN1 was output directly using the history output function of ABAQUS. The distribution of the rivet load under different loads was plotted for joints with different buttress gaps, as shown in Figure 17.

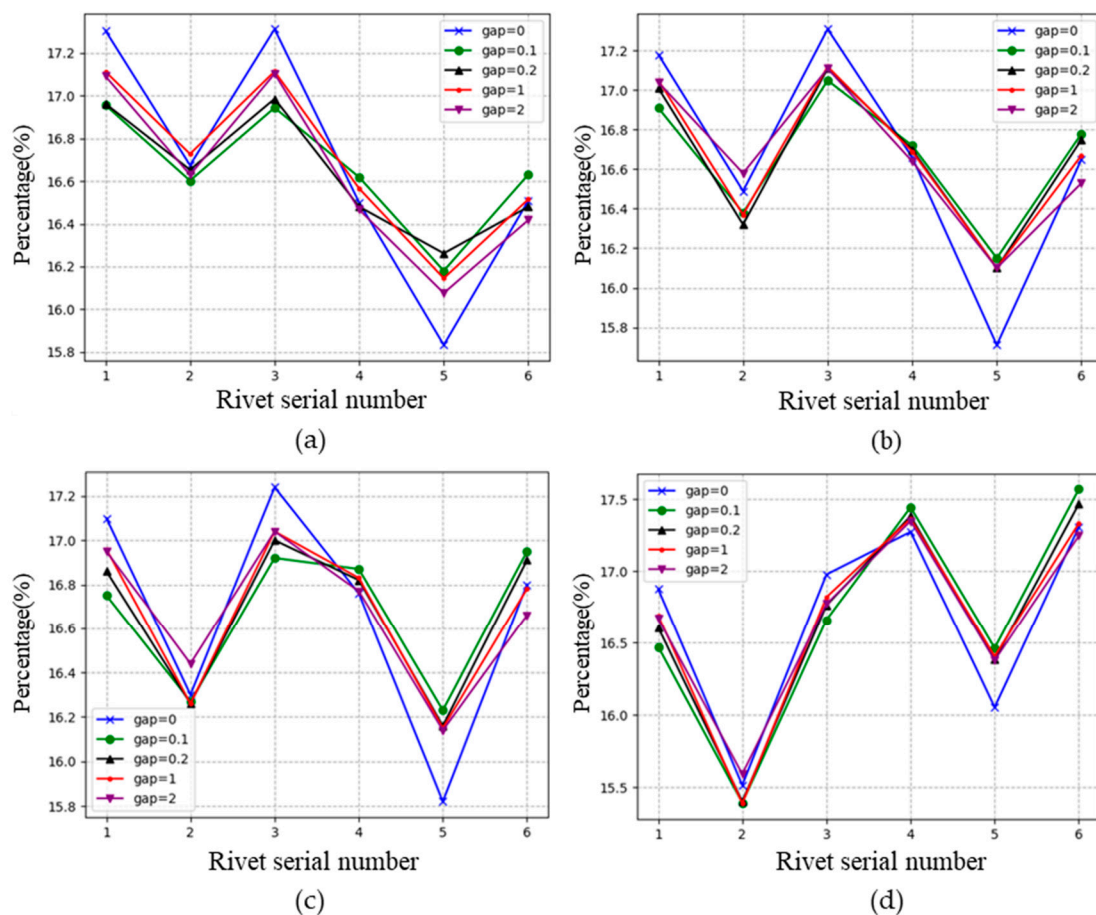


**Figure 17.** Distribution of rivet loads under different tensile loads: (a) Tensile load on 1 KN; (b) Tensile load on 3 KN; (c) Tensile load on 10 KN; (d) Tensile load on 25 KN. (Units of gap: mm).

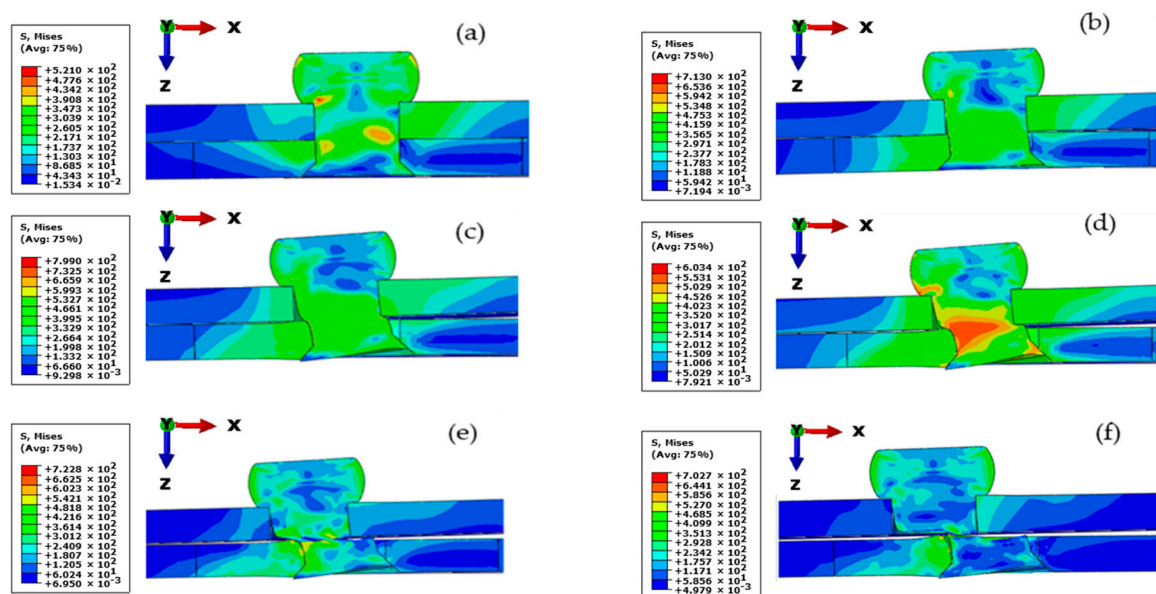
As can be seen in Figure 17, when the butt gap value is greater than 0.1 mm, the rivet loads are approximately the same for each of the joints with different butt gaps. At low loads, the rivet loads are greater for No. 1 and No. 3 rivets and less for No. 5 rivets; as the applied load increases, the rivet loads show approximately the same trend for joints with a 0 seam gap as for joints with a seam gap between 0.1 and 2 mm. The difference in rivet load ratio between rivets in the same position during tension is approximately 0.2% for joints with a butt gap of 0.1 to 2 mm, and the rivet load ratio is approximately the same.

From the previous analysis of the wall sheet stress distribution in 3.2.1, it can be seen that at lower tensile loads, the joint with a wall sheet gap of 0 is subjected to additional squeezing forces. From the analysis of the deformation of the joint, it is known that the stress distribution of the wall sheet is not uniform, the compressive stress in the middle position is greater than the compressive stress on both sides. As the tensile load increases, the squeezing force between the wall sheets gradually decreases. Therefore, at a lower

tensile load, the joint with a 0 gap between the wall sheet and the No. 1 and No. 3 rivets has a greater rivet load. When the tensile load gradually increases, at this point the wall plates are no longer in contact with each other, and the rivet load distribution for joints with a gap of 0 is similar to that for joints with a gap of 0.1 to 2 mm. For the joints with a wall sheet gap of 0.1 to 2 mm, the stresses on the joints and the stress distribution are the same and the rivet load ratio is therefore approximately the same.

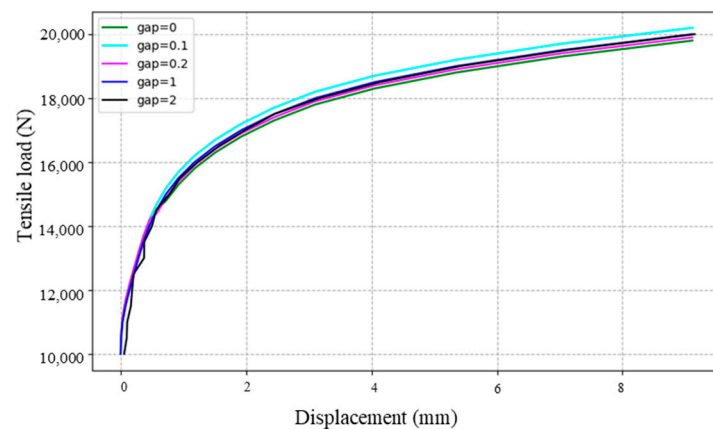
### 3.2.4. Failure Analysis of Single-Strap Riveted Joints

Figure 18 is the failure process of the riveted joint during tensile process. At this time, the shear failure of the rivet occurs. Shear fracture refers to the fracture along the action surface of the maximum shear stress. In the whole process of shear fracture, a group of inclined tensile cracks are first generated. With the increase of stress, these tensile cracks penetrate each other, and then form a penetrating shear surface, which eventually leads to the final shear fracture. As we can see in Figure 18, the rivet head is separated from the tail, the rivet head continues to remain in the wall sheet, and there is a small amount of material sliding in the tensile direction. The panel itself does not break, but it will produce severe plastic deformation in the tensile direction. Due to the extrusion effect of the sink on the panel during stretching, large deformations will also occur at the countersink of the wall sheet nail hole due to the squeezing effect of the countersunk head on the wall sheet during tension.



**Figure 18.** Shear failure process of rivet. (Unit: MPa). (a) Riveting completed. (b) Shear starting. (c) Deformation of rivet. (d) Significant stress concentration. (e) Rivet obvious deformation. (f) Shear fracture of rivet.

The failure mode of plate is fracture failure of rivet. Since the linear load is applied in the simulation, that is, the X-direction shear force applied to the wall clamping part increases linearly with time. Therefore, the simulation model in this paper can simulate the tensile fracture process of the test piece. The load displacement curves for the strap sheet joint with different butt gap were plotted as shown in Figure 19. It can be seen that the difference in load-displacement curves of the strap sheet joints with different counter seam gap is small and the counter seam gap of the strap sheet joints does not have a significant effect on the joint quality of the joints.



**Figure 19.** Load displacement curves for strap sheet joints with different gaps.

#### 4. Conclusions

In the case of the single-strap riveted joints, there is a seam gap between the adjacent sheets. If the joint has a small gap, the adjacent sheets may contact each other after the riveting is completed. The mutual extrusion between the sheets will cause additional initial stress, thus affecting the stress distribution of the sheets. When the gap between the sheets increases, there will be no contact between the wall sheets after riveting. It should be noted that the value of the gap between the sheets should not be too large, otherwise it will affect the structural size of the entire component.

When tension is carried out under low-strength load, the left and right sheets of the riveted joint model with a gap of zero will contact and squeeze during tension, resulting in additional compressive stress. As the load applied to the wall sheets continues to increase, the strap and wall sheets bend and deform due to the secondary bending action, and no further contact action occurs between the sheets. When the gap is greater than 0, the interplate extrusion decreases significantly, so the effect of the gap between sheets on the quality of joints is not obvious. The quality of riveted joints may be related to the thickness of the plate, the diameter of the rivet and other factors, which need to be further investigated.

**Author Contributions:** Conceptualization, Z.K. and Y.B.; Methodology, Z.Z. and Y.Z.; Software, C.Z.; Validation, Y.L. and Y.Z.; Formal analysis, Y.L. and Z.K.; Investigation, Z.Z. and Y.L.; Resources, Y.B.; Data curation, Z.Z. and Y.L.; Writing—original draft preparation, Y.L.; Writing—review and editing, Z.K. and Y.B.; Visualization, Z.Z.; Supervision, Z.K. and Y.B.; Project administration, Y.B.; Funding acquisition, Y.B. All authors have read and agreed to the published version of the manuscript.

**Funding:** This research was funded by National Natural Science Foundation of China (No. 51775495), Key Projects of the National Natural Science Foundation of China (No.: 91748204) and Educational Commission of Zhejiang Province of China (No.: 188310-542122/002/006).

**Institutional Review Board Statement:** Not applicable.

**Informed Consent Statement:** Not applicable.

**Data Availability Statement:** Data is contained within the article.

**Acknowledgments:** The authors would like to thank Jintong Liu and Qiwei Huang for their technical help in the research.

**Conflicts of Interest:** The authors declare no conflict of interest.

#### References

- Skorupa, A.; Skorupa, M.; Machniewicz, T.; Korbel, A. Fatigue crack location and fatigue life for riveted lap joints in aircraft fuselage. *Int. J. Fatigue* **2014**, *58*, 209–217. [[CrossRef](#)]
- Liang, Q.; Zhang, T.; Zhu, C.; Bi, Y. Effect of riveting angle and direction on fatigue performance of riveted lap joints. *Coatings* **2021**, *11*, 236. [[CrossRef](#)]

3. Cabrera-Gonzalez, J.A.; Vargas-Silva, G.; Barroso, A. Riveted joints in composites, a practical tool to estimate stresses around the rivet hole. *Compos. Struct.* **2021**, *263*, 113735. [[CrossRef](#)]
4. Anasori, B.; Saillot, F.; Stanley, D.; Awerbuch, J.; Tan, T. Fatigue crack growth in aluminum lithium riveted lap joints. *Procedia Eng.* **2014**, *74*, 413–416. [[CrossRef](#)]
5. Yu, H.; Zheng, B.; Xu, X.; Lai, X. Residual stress and fatigue behavior of riveted lap joints with various riveting sequences, rivet patterns, and pitches. *Proc. Inst. Mech. Eng. Part B J. Eng. Manuf.* **2019**, *233*, 2306–2319. [[CrossRef](#)]
6. Wang, H.; Ceglarek, D. Variation propagation modeling and analysis at preliminary design phase of multi-station assembly systems. *Assem. Autom.* **2009**, *29*, 154–166. [[CrossRef](#)]
7. Braden, P. Fatigue Damage Detection for Advanced Military Aircraft Structures. In *2016 IEEE Autotestcon*; Institute of Electrical and Electronics Engineers Inc.: Anaheim, CA, USA, 2016.
8. Cheng, L.; Wang, Q.; Li, J.; Ke, Y. Propagation analysis of variation for fuselage structures in multi-station aircraft assembly. *Assem. Autom.* **2018**, *38*, 67–76. [[CrossRef](#)]
9. Szolwinski, M.P.; Farris, T.N. Linking riveting process parameters to the fatigue performance of riveted aircraft structures. *J. Aircr.* **2000**, *37*, 130–137. [[CrossRef](#)]
10. Atre, A.; Johnson, W.S. Analysis of the effects of interference and sealant on riveted lap joints. *J. Aircr.* **2007**, *44*, 353–364. [[CrossRef](#)]
11. Aman, F.; Cheraghi, S.H.; Krishnan, K.K.; Lankarani, H. Study of the impact of riveting sequence, rivet pitch, and gap between sheets on the quality of riveted lap joints using finite element method. *Int. J. Adv. Manuf. Technol.* **2013**, *67*, 545–562. [[CrossRef](#)]
12. Manes, A.; Giglio, M.; Vigano, F. Effect of riveting process parameters on the local stress field of a T-joint. *Int. J. Mech. Sci.* **2011**, *53*, 1039–1049. [[CrossRef](#)]
13. Kumar, D.V.T.G.; Naarayan, S.S.; Sundaram, S.K.; Chandra, S. Further numerical and experimental failure studies on single and multi-row riveted lap joints. *Eng. Fail. Anal.* **2012**, *20*, 9–24. [[CrossRef](#)]
14. Liu, J.; Zhao, A.; Ke, Z.; Li, Z.; Bi, Y. Investigation on the residual stresses and fatigue performance of riveted single strap butt joints. *Materials* **2020**, *13*, 3436. [[CrossRef](#)] [[PubMed](#)]
15. Cheraghi, S.H. Effect of variations in the riveting process on the quality of riveted joints. *Int. J. Adv. Manuf. Technol.* **2008**, *39*, 1144–1155. [[CrossRef](#)]
16. Lei, C.; Bi, Y.; Li, J. Continuous numerical analysis of slug rivet installation process using parameterized modeling method. *Coatings* **2021**, *11*, 189. [[CrossRef](#)]
17. Gray, P.J.; McCarthy, C.T. A highly efficient user-defined finite element for load distribution analysis of large-scale bolted composite structures. *Compos. Sci. Technol.* **2011**, *71*, 1517–1527. [[CrossRef](#)]
18. McCarthy, M.A.; Lawlor, V.P.; Stanley, W.F.; McCarthy, C.T. Bolt-hole clearance effects and strength criteria in single-bolt, single-lap, composite bolted joints. *Compos. Sci. Technol.* **2002**, *62*, 1415–1431. [[CrossRef](#)]
19. Lei, C.; Huang, Q.; Bi, Y. Tensile load distribution improvement of three-row riveted lap joint based on different squeezing displacement combinations. *Coatings* **2021**, *11*, 856. [[CrossRef](#)]
20. Li, G.; Shi, G.; Bellinger, N.C. *Residual Stress/Strain in Three-Row, Countersunk, Riveted Lap Joints*; American Institute of Aeronautics and Astronautics Inc.: Reston, VA, USA, 2007; pp. 1275–1285.
21. Jun, Q.Y.; Zhong, Q.W.; Yong, G.K.; Ning, L. Finite element analysis of axis deviation between rivet and plate hole. *Appl. Mech. Mater.* **2013**, *321*, 2388.
22. Pan, M.H.; Tang, W.C.; Xing, Y.; Ni, J. Numerical simulation analysis for deformation deviation and experimental verification for an antenna thin-wall parts considering riveting assembly with finite element method. *J. Cent. South Univ.* **2018**, *25*, 60–77. [[CrossRef](#)]
23. Liu, Y.; Li, H.; Zhao, H.; Liu, X. Effects of the die parameters on the self-piercing riveting process. *Int. J. Adv. Manuf. Technol.* **2019**, *105*, 3353–3368. [[CrossRef](#)]
24. Gray, P.J.; McCarthy, C.T. A global bolted joint model for finite element analysis of load distributions in multi-bolt composite joints. *Compos. Part B Eng.* **2010**, *41*, 317–325. [[CrossRef](#)]